Nat Neurosci. 2016 May;19(5):734-41. doi: 10.1038/nn.4274. Epub 2016 Mar 28.

Agouti-related peptide neural circuits mediate adaptive behaviors in the starved state.

Padilla SL[1], Qiu J[2], Soden ME[3], Sanz E[4], Nestor CC[2], Barker FD[1], Quintana A[4], Zweifel LS[3], Rønnekleiv OK[2,5], Kelly MJ[2,5], Palmiter RD[1].

http://www.nature.com/neuro/journal/v19/n5/full/nn.4274.html

This is the Accepted Manuscript of an article published in "Nature Neuroscience", 2016, Vol. 19, No. 5, p. 734-741. DOI: 10.1038/nn.4274□□

Available at: http://dx.doi.org/10.1038/nn.4274□□

AgRP Neural Circuits Mediate Adaptive Behaviors in the Starved State

Stephanie L. Padilla, Jian Qiu, Marta E. Soden, Elisenda Sanz, Casey C Nestor, Forrest D. Barker, Albert Quintana, Larry S. Zweifel, Oline K. Rønnekleiv, Martin J. Kelly and Richard D. Palmiter

In the face of starvation animals will engage in high-risk behaviors that would normally be considered maladaptive. Starving rodents for example will forage in areas that are more susceptible to predators and will also modulate aggressive behavior within a territory of limited or depleted nutrients. The neural basis of these adaptive behaviors likely involves circuits that link innate feeding, aggression, and fear. Hypothalamic AgRP neurons are critically important for driving feeding and project axons to brain regions implicated in aggression and fear. Using circuit-mapping techniques, we define a disynaptic network originating from a subset of AgRP neurons that project to the medial nucleus of the amygdala and then to the principle bed nucleus of the stria terminalis, which plays a role in suppressing territorial aggression and reducing contextual fear. We propose that AgRP neurons serve as a master switch capable of coordinating behavioral decisions relative to internal state and environmental cues.

Seminal ecological studies reveal that prey species display cost-benefit decision making when foraging for food. The costs of foraging include the energy demands associated with food seeking along with environmental threats such as predators and thermal challenges. To maximize fitness, many prey species forage within a familiar territory, in zones that are relatively protected from predators and have moderate temperatures [1-3]. However, when challenged with starvation, the behavioral priorities associated with foraging adapt and prey species display higher-risk behavior to find food [4-7].

Territorial species protect their home domain from conspecifics using aggression, ranging from threat displays to outright attacks; in this manuscript we define territory as a defended area. There are data to support that food is the ultimate resource governing territorial defensive behaviors [3]. In the absence of food, group-housed *Drosophila* display relatively little aggression; however, when presented with food, flies will fight to obtain nutrients [8]. This behavior change, in the presence or absence of food, exemplifies a complex decision associated with the cost of exerting energy to challenge a competitor relative to the benefit of a food reward.

Orexigenic AgRP neurons are active in a starved state [9, 10] and elicit signals that are paramount to the sensation of hunger [11-13]. Coined for the expression of agouti-related peptide (AgRP), AgRP neurons are inhibitory projections neurons; they are GABAergic and express two inhibitory neuropeptides, neuropeptide Y (NPY) and AgRP [9, 14-16]. Somewhat paradoxically, AgRP neurons appear to stimulate hunger by inhibiting downstream brain regions involved in satiety. Immediate early gene expression and *in vivo* imaging studies demonstrate that most AgRP neurons are active in the fasted state, yet this population is both anatomically and functionally heterogeneous[17 18]. AgRP neurons are derived from at least two progenitors [19] and project (with minimal collaterals) to approximately 15 unique downstream brain regions [15, 17]. Activation of distinct AgRP projections revealed a “parallel and redundant” network of satiety centers downstream of AgRP, but interestingly, some AgRP target regions do not evoke a feeding response [17]. We propose that the heterogeneous AgRP population functions to coordinate

numerous behavioral and physiological adaptations that prioritize food seeking and energy conservation under conditions of starvation.

AgRP neurons may influence behavioral decisions by signaling to brain regions that are involved in sensory processing. For example, a subset of AgRP neurons project to the medial amygdala (MeA) [15, 20, 21], a brain region implicated in innate social behaviors including aggression [22]. Chemosensory cues of conspecific mice activate cells in the MeA, as indicated by the expression of Fos [23, 24], and acute activation of GABAergic cells in the posterior dorsal MeA can induce attack behavior [25]. Under conditions of starvation, AgRP signaling to the MeA may alter an animal's normal response to chemosensory cues, shifting behavior away from protecting an energy-depleted territory and toward exploratory, food-seeking behavior. To test this idea, we used a combination of viral and genetic tools to activate AgRP neurons, and compared the behavior of these mice to those in the fasted state. We describe a specific starved-state neural circuit that influences innate and learned behavioral responses (**Supplementary Fig. 1**).

RESULTS

AgRP neuronal activation promotes risk taking and reduces territorialism.

In the wild/natural state, starvation influences foraging behavior such that prey species, in particular rodents, are willing to forage in: 1) areas that are more exposed to predators, 2) areas that pose a thermal challenge, and/or 3) novel areas outside of the habitual foraging zone [4]. To model this behavioral adaptation in a laboratory setting, we designed an experiment that requires mice to forage in an arena that they are conditioned to avoid. We used Pavlovian conditioning to instate a context-dependent fear for one side of a two-chamber arena. The chambers of the arena contain distinct floor texture, visual cues, and odors. During conditioning, mice learned to associate one chamber with a paired foot shock (**Fig. 1a**). We observed that, under normal conditions, mice will develop an aversion to

48 the shock-associated side, spending only 24.5 ± 2.5% of the 30-min trial in this chamber post-
49 conditioning. Fasted animals, however, overcame the conditioned threat and spent more than 40% of
50 the time in the shock-associated side. During habituation and training, food was present below the floor
51 grid in the shock-associated chamber. On test day, the food either remained under the floor grid (food-
52 blocked group), or was presented in the chamber and available for consumption (food-access group).
53 The food-access group spent 46.9 ± 4.6% of the trial in the shock chamber; similarly, the food-blocked
54 group spent 43.2 ± 1.6% of the trial in the shock chamber (**Fig. 1d**, black outlined bars; **Supplemental**
55 **STATISTCS provides details of all tests performed**). We questioned whether the fasted state or the food
56 cues biased this experimental paradigm. To validate that the conditioned avoidance could be acquired in
57 fasted animals we repeated the assay in the absence of food. We found that similar to fed controls,
58 fasted animals avoided the shock-associated chamber, spending only 25.7 ± 4.7 % of the trial in the
59 shock chamber (**Supplementary Fig. 2a**).

60 We hypothesized that high-risk foraging is facilitated by a neural circuit that alters the behavioral
61 state during starvation. Given that AgRP neurons are active in the fasted state, we reasoned that they
62 may promote high-risk exploration. We made AgRP neurons excitable by transducing *Agrp*^{Cre} mice with
63 the stimulatory DREADD (designer receptor exclusively activated by designer drugs), hM3Dq [26], via viral
64 delivery of AAV1-DIO-hM3Dq:mCherry into the arcuate hypothalamic nucleus (ARH); control mice
65 received AAV1-DIO:mCherry virus (**Fig. 1b, c**). The designer receptor ligand, clozapine-n-oxide (CNO),
66 induces Gαq-mediated signal transduction, thereby activating the AgRP neurons [12]. Using this model, we
67 exposed AgRP neuron-stimulated mice to the food-challenge test described above. Similar to fasted
68 animals, we found that AgRP neuron-stimulated mice spent more time in the shock-associated chamber
69 relative to controls. Both food-available and food-blocked groups spent 40.0 ± 5.6% and 45.6 ± 5.6% of
70 the trial in the shock chamber, respectively; while control animals displayed an aversion to the shock-
71 associated side and spent only 22.7 ± 3.2% of the trial in this chamber (**Fig. 1d**, red bars). These data

support that, beyond promoting food intake, AgRP neurons can influence the behavioral response to environmental threats.

In a second test, we evaluated innate anxiety-like behavior by assessing the willingness of animals to enter an exposed platform on an elevated maze. In support of previous literature [27], both fasted and AgRP neuron-stimulated animals spent significantly more time in the exposed platforms compared to controls (**Fig. 1e**). AgRP neuron-stimulated mice are reported to exhibit enhanced locomotor activity [12] and, consistent with this, we found that during the maze trial, stimulated mice moved an average total distance of 3148 ± 148.3 cm, while controls moved an average of 2024 ± 186.5 cm. Considering this potential confound, we analyzed the percent of distance traveled in the exposed arms. Consistent with our previous results, stimulated mice traveled more in the open arms compared to controls (stimulated, 48.2 ± 3.1%; controls, 30.7 ± 4.5%).

In the state of starvation, the costs associated with foraging are not limited to environmental threats, but also include the threat of dwindling energy reserves. As a reflection of this, organisms forage in a way that minimizes the energy costs associated with food seeking [1-3, 28]. For example, territorial-defense behavior is not an efficient use of energy if a territory is depleted of resources [8]. Experimentally, we evaluated territorial behavior using the resident-intruder assay. Resident males were sexually experienced and territorialized to an isolated home cage; they were evaluated for aggressive territorial behaviors including: holding, fighting (boxing/attacking/mounting), high-speed chasing, and nudging. The intruders were sexually naïve, group-housed littermates that were younger, and smaller than the resident animals (**Supplementary Fig. 2b**). Compared to the fed state, fasted animals displayed less home-cage aggression toward an intruder (**Fig. 1f**, black bars). In this manuscript we used a 48 hr fast to maximally activate the feeding circuits; however, we found that 24-hr fasted residents also displayed decreased home-cage aggression (**Supplementary Fig. 2c**). We also observed that fasted

residents spent significantly more time investigating the snout of the intruder—perhaps smelling food odorants on the intruder's snout—along with displaying escape behaviors including rearing and jumping (**Supplementary Fig. 2b-d**). To control for changes in aggression upon repeated exposure, the order of the baseline-state test was randomized and unique intruders were used in every trial. We did not observe intruder-initiated aggression toward resident animals.

To test the role of AgRP neurons in fasting-related territorial behavior, we evaluated hM3Dq-transduced *Agrp*^{Cre} animals (injected with either saline or CNO) in the resident-intruder assay. Similar to fasting, AgRP neuron-stimulated mice displayed less home-cage aggression toward an intruder (**Fig. 1f**, red bars). If food was presented during the trial, AgRP neuron-stimulated residents spent the majority of the trial engaged with the food, eating 0.34 ± 0.03 g of food during the 10-min trial (**Supplementary Fig. 3**).

AgRP neuron projections to the MeA affect feeding and territorialism

Neurons in the MeA are involved in innate social behavior, including territorialism. We reasoned that the inhibitory AgRP^{MeA} circuit may be responsible for starved-state decreases in territorial aggression. AgRP-immunoreactive fibers have been observed in the MeA [15], but the function of the MeA-projecting AgRP population (AgRP^{MeA}) has yet to be defined. To test whether AgRP fibers in the MeA make direct inhibitory connections to cells in this region, we transduced *Agrp*^{Cre}-expressing mice with a conditional channelrhodopsin-2 (ChR2)-expressing virus [29], AAV1-DIO-ChR2:YFP (**Fig. 2a**). We photostimulated AgRP fibers in the MeA and performed whole-cell recordings in slice preparations. MeA soma in close proximity to fluorescent AgRP fibers were patched; 4 of 11 cells from 2 mice displayed a light-evoked inhibitory post-synaptic current (IPSC) that was blocked by the $GABA_A$ receptor antagonist picrotoxin (PTX) but not by glutamate receptor antagonists (**Fig. 2b**). We used retrograde tracing to quantify the subset of AgRP^{MeA}-projecting neurons. Fluorescent RetroBeads injected into the MeA (**Supplementary**

Fig. 4a) were retained in 7.1 ± 0.6 % of AgRP-expressing cells (167 ± 15 of 2356.3 ± 146 total hemisphere, *n* = 3; **Fig. 2c, d**). These data establish that a subset of AgRP neurons make direct inhibitory connections onto MeA neurons.

In lieu of a genetic marker to define the subpopulation of $AgRP^{MeA}$ neurons, we used optogenetic fiber stimulation to probe this anatomically distinct AgRP circuit (**Fig. 2e, f; Supplementary Fig. 4b**). Similar to fasting, $AgRP^{MeA}$ fiber-stimulated animals displayed less home-cage aggression relative to a non-stimulated baseline state (**Fig. 2g**). To gauge the specificity of the $AgRP^{MeA}$ circuit on territorial behavior, we stimulated AgRP neurons that project to the PVH. Prior studies demonstrated that the $AgRP^{PVH}$ circuit can induce maximal food intake equivalent to that observed following a fast [30]. If fasting-induced territorial behavior is a consequence of being hungry, then this circuit should also modulate home-cage aggression. We did not observe a significant change in home-cage aggression upon $AgRP^{PVH}$ stimulation (**Fig. 2e, f; Supplementary Fig. 4c**). Together, these data indicate that distinctly projecting AgRP neurons can mediate unique behaviors.

Along with social behavior, there is evidence suggesting that the MeA is also involved in feeding behavior and body-weight regulation [31-33]. We found that $AgRP^{MeA}$ fiber-stimulated mice ate significantly more than non-stimulated, fiber-attached controls (0.87 ± 0.12 g vs 0.10 ± 0.02 g; **Fig. 2h**). To gauge the relative magnitude of this effect, we measured light-evoked food intake from $AgRP^{PVH}$ fibers. Under comparable conditions, the hyperphagia induced by $AgRP^{PVH}$ fiber stimulation was 2.5-fold higher than $AgRP^{MeA}$ fiber stimulation (**Fig. 2h**). These data add to growing evidence that there are parallel and redundant AgRP circuits involved in feeding behavior [17].

Manipulating cells downstream of AgRP in the MeA

AgRP neurons co-express NPY and AgRP [9, 15] and, therefore, post-synaptic targets of AgRP neurons likely express receptors for these neuropeptides including NPY 1 or 5 receptors (Npy1R or Npy5R) [34] and the

melanocortin 4 receptor (MC4R). To evaluate the function of MeA cells that receive information from AgRP neurons, we generated an *Npy1r*^{Cre} knock-in mouse line (**Fig. 3a**).

We validated the correct targeting of this knock-in using multiple approaches. Prior to injection, neomycin-resistant ES cell colonies were screened for the proper insertion of *Cre* in the targeted *Npy1r* allele by Southern blot analysis. We also evaluated transcripts expressed in *Npy1r*^{Cre} cells by crossing this line to a Cre-dependent RiboTag mouse that expresses an epitope-tagged ribosomal protein (RPL22:HA) [35]. The conditional expression of the tagged ribosomes in Cre-positive cells provided a means to isolate mRNA transcripts from these cells. *Npy1r*^{Cre}-RiboTagged cells in the MeA (**Fig. 3b**) were enriched in both *Npy1r* and *Cre* transcripts relative to transcripts expressed in all cells within the same region (**Fig. 3c**). These experiments confirmed the positional insertion of *Cre* in the *Npy1r* allele by Southern blot and demonstrated that *Cre* is expressed in Npy1R cells in the MeA (Npy1R^{MeA}) using RiboTag technology.

To further profile the Npy1R^{MeA} cells, we mined the RiboTag-isolated transcriptome, probing for genes characteristic of excitatory, inhibitory and glial cells. We found that Npy1R-RiboTagged cells were enriched for both *Mc4r* and *Gad2* transcripts. The glutamate transporter, *Slc17a6* (Vglut2) was not enriched and the glial cell marker, *Cnp* was de-enriched (**Fig. 3c**). These data indicate that Npy1R cells in the MeA may be inhibitory neurons, an idea explored in more detail below.

Npy1R^{MeA} cells are anatomically distributed throughout the MeA, with a slightly biased distribution in the anteroventral subdivision (**Fig. 3d** and **Supplementary Fig. 5**), a pattern that resembles *Mc4r* expression [20, 21]. To investigate whether Npy1R^{MeA} cells are involved in feeding behavior or aggression, we bilaterally transduced the MeA of *Npy1r*^{Cre} mice with AAV1-DIO-hM3Dq:YFP (**Fig. 3e**). Because inhibitory AgRP^{MeA} fiber stimulation decreased territorial aggression, we predicted that activation of target Npy1R neurons would have the opposite effect. In line with this idea, we found that CNO-induced Npy1R^{MeA} neuron activation significantly increased home-cage aggressive behavior (**Fig. 3f and**

Supplementary Movie 1). Consistent with previous work using pharmacogenetics to manipulate social behavior [25], we observed a scale of aggressive phenotypes upon CNO-induced activation. Four of nine stimulated animals displayed overt attack behavior, while the rest engaged in other aggressive behaviors including, nudging, aggressive grooming, and holding. To determine the degree of aggression evoked, we evaluated the overtly aggressive males in the presence of an anesthetized intruder; all of these mice attacked the anesthetized conspecific within 59.0 ± 5.9 s (**Supplementary Movie 2**), a behavior never observed in non-stimulated mice. Along with changes in aggression, activation of the Npy1R^{MeA} neurons significantly decreased food consumption within the first 4 h of the dark cycle (**Fig. 3g**).

To determine the necessity of the Npy1R^{MeA} population for satiety, territorial aggression, and high-risk exploration, we used a viral approach to chronically inhibit *Npy1r^{Cre}*-expressing cells in the MeA. Tetanus toxin light chain prevents synaptic transmission [36] and AAV1-DIO-GFP:TetTox (**Fig. 3h**) has been used to silence Cre-expressing neurons [37]. In the food-challenge assay, TetTox-silenced Npy1R^{MeA} mice spent more time in the shock-associated chamber post-conditioning (**Fig. 3i**). They also gained significantly more weight after viral transduction relative to controls (**Fig. 3j**), but there was no statistical difference between TetTox-silenced mice relative to controls in territorial aggression (**Fig. 3k**). Given that acute inhibition from AgRP^{MeA} fibers was sufficient to suppress home-cage aggression, this finding was surprising but may be the result of compensatory plasticity following chronic inhibition. We also evaluated anxiety using the elevated plus maze. There was no difference in open-arm exploration between TetTox-silenced mice relative to YFP controls (17.2 4.2% for TetTox versus 21.2 3.1% for YFP controls, P = 0.5; **Supplementary Fig. 6**).

A disynaptic network from ARH^{AgRP} to the MeA^{Npy1R} and on to the pBNST

To identify candidate secondary targets of the AgRP → MeA circuit, we mapped the projection field of Npy1R^{MeA} cells using a virus expressing a Cre-dependent, synapse-specific reporter (AAV1-DIO-synaptophysin:YFP**, Fig. 4a**). We observed dense reporter expression in the posterior principle region of the bed nucleus of the stria terminalis (pBNST), along with several other brain regions including the lateral hypothalamic area, periaqueductal grey, parabrachial nucleus, ventromedial hypothalamus and anterior olfactory bulb (**Fig. 4b**). To determine whether these were secondary targets of AgRP neurons, we injected a Cre-dependent and trans-synaptic anterograde tracing virus, H129Δ-fs-TK-TT [38], into the ARH of *Agrp^{Cre}* animals (**Fig. 4c**). TdTomato fluorescence was observed in many sites throughout the brain, notably the MeA and the pBNST (**Fig. 4c**).

The pBNST is an established target of the MeA [39, 40] and while AgRP fibers have been found in the anterior BNST [15, 17], they have not been observed in the pBNST. Consistent with this observation, we observed few, if any, fluorescent cell bodies in the ARH following injection of fluorescent RetroBeads into the pBNST (**Supplementary Fig. 7a, b**). To test the idea that the pBNST is a secondary target of AgRP neurons via the MeA, we co-injected RetroBeads into the pBNST and H129Δ-fs-TK-TT into the ARH of *Agrp^{Cre}* mice (**Supplementary Fig. 7c, d**). We observed expression of both reporters in the MeA (**Fig. 4d**), consistent with the idea that the pBNST is a secondary target of the AgRP → MeA circuit (**Fig. 4e**). Due to the nature of H129 infection, the cells were not healthy enough to quantify the overlap of these reporters in the MeA. Instead, we use an alternative approach to further characterize the properties of cells in the MeA that receive input from AgRP neurons and project to the pBNST.

Numerous cell types in the posterior MeA have been defined based on electrophysiological and morphological properties [41-43]. To investigate the properties of pBNST-projecting MeA neurons we injected RetroBeads into the pBNST and performed whole-cell recordings on bead-labeled cells in the MeA (**Fig. 5**). When subjected to current-step injections, we observed a prominent hyperpolarization-

activated voltage sag (h-current, denoted by the arrow, in 10 of 13 cells recorded), which has been described in type 1 GABAergic projections neurons in the posterior MeA [43]. In addition, we discovered that that a subset of these neurons expressed a T-type calcium current (denoted by the arrow head, in 7 of 13 cells; **Fig. 5c**).

We previously determined that AgRP neurons can evoke GABA-mediated IPSCs in MeA neurons. Using the RetroBead labeling described here, we sought to determine whether ChR2-expressing AgRP neurons could evoke light-induced responses in pBNST-projecting MeA cells (**Fig. 5a, b**). Bead-positive MeA soma in proximity to YFP fibers demonstrated light-evoked IPSPs in 3 of 11 recorded cells (**Fig. 5d**). Similar to the recordings in **Fig 2b**, the light-evoked inhibitory response occurred with a short latency to the photostimulation, suggesting a direct connection. To further support this idea, we identified a shifted (smaller and longer latency) light-evoked IPSP in the presence of the action-potential blocker, TTX along with a potassium channel blocker, 4-aminopyridine (4-AP)—a property indicative of monosynaptic connections in ChR2-assisted circuit mapping (**Fig. 5d, red trace**) [44].

We used pharmacology in the slice preparation to demonstrate that light-responsive, bead-positive cells in the MeA also respond to NPY. Bath application of NPY in the presence of TTX resulted in an outward current when held at a membrane potential of -60 mV in 4 out of 4 cells tested (**Fig. 5e**). To investigate the NPY-induced current, voltage ramps were performed in the presence and absence of NPY (**Fig. 5f**). Consistent with the idea that NPY-induced current is mediated by G protein-coupled inwardly-rectifying potassium channel activation [45, 46], we found that the reversal potential for the outward current was at -85 mV, close to the Nernst equilibrium potential for potassium.

Based on the firing properties recorded in bead-positive cells (**Fig. 5c**) along with enrichment of *Gad2* in Npy1R-RiboTagged cells (**Fig. 3c**), we predicted that these neurons were GABAergic[43]. Following recording, we harvested the cytosol of the cells [47] and performed single-cell PCR to test for *Slc32a1*

(Vgat) expression. The majority of cells were Vgat-positive—out of 11 successfully harvested *Actb*-positive cells, 7 tested positive for Vgat expression, while the remaining 4 did not amplify either Vgat or Vglut templates (**Fig. 5g**). Together, our data are consistent with the idea that a subset of AgRP neurons synapse on a population of inhibitory, NPY-responsive cells in the MeA that project to the pBNST.

The behavioral influence of the ARH^{AgRP} → MeA^{Npy1R} → pBNST circuit

The $Npy1R^{MeA}$ population projects to numerous efferent targets, some of which have been implicated in aggressive behavior, including the VMH and PAG [24, 48]. Because AgRP neurons make a disynaptic connection to the pBNST via the MeA, we hypothesized that this circuit may be involved in aggressive/territorial behaviors. To investigate the role of pBNST-projecting $Npy1R^{MeA}$ neurons, we virally transduced *Npy1r*^{Cre} mice unilaterally with AAV1-DIO-ChR2:YFP virus and placed fiber optic a cannula above either the ipsilateral VMH or pBNST (**Fig. 6a**). Optogenetic stimulation of $Nyp1R^{MeA}$ fibers in the pBNST evoked significantly more territorial defensive behavior (**Fig. 6b**). However, rather than overt attack behavior, the pBNST fiber stimulation increased nudging activity; the resident mouse followed the intruder for the majority of the assay, constantly nudging the intruder into the wall of the cage (**Supplementary Movie 3**). As opposed to violent aggression, a nudging threat display may be adequate for territorial defense from most competitors (**Supplementary Fig. 7e**). It should also be noted that the methods of stimulation in these two instances were different. We activated $Npy1R^{MeA}$ soma using metabotropic hM3Dq DREADD receptors while we stimulated the $Npy1R^{MeA}$ fibers in the pBNST using ionotropic photostimulation; hence, we cannot exclude the possibility that this difference accounts for the behavioral difference.

Optogenetic stimulation of $Npy1R^{MeA}$ fibers in the VMH did not result in significant differences in territorial aggression (**Fig. 6b**). We also measured the effect of photostimulating $Npy1R^{MeA}$ efferents in the pBNST or VMH on food intake, but did not observe a significant effect of stimulating either of these

projections (**Fig. 6c**). Because Npy1R neurons project to numerous downstream targets, it is likely that the overt/violent aggression observed following Npy1R^{MeA} neuron stimulation (**Fig. 3f and Supplementary Movie 1,2**), and also feeding behavior (**Fig. 3g**) are orchestrated by projections to targets other than the pBNST or VMH. The modulatory effect of AgRP^{MeA} fiber stimulation on territorial behavior likely involves Npy1R neurons that project to the pBNST, a circuit that can be modulated under physiological conditions of negative energy balance.

DISCUSSION

Risk assessment and territorialism require sensory processing of environmental cues. Rodents select a territorial domain for nesting and foraging with respect to the risk of predation and will defend the limited resources of this area from conspecific intruders. However, under conditions of starvation, mice take more risks to forage in exposed or threatening areas and are less willing to defend a territory that is depleted of resources, exemplifying a behavioral adaptation that is associated with an internal state change [49]. We explored the influence of AgRP neurons in these starvation-related decisions. Similar to fasted animals, acute activation of AgRP neurons was sufficient to induce food seeking in a threatening environment and decrease territorial defense behavior. AgRP neurons send axonal projections to downstream brain regions involved in sensory processing; hence, we propose that in the state of starvation, these neurons tune behavioral and physiological processes to conserve energy and prioritize food acquisition.

Both territorial aggression and the activation state of AgRP neurons depend on the availability of food. Hungry animals will aggressively defend limited food resources from competitors. However, if food is depleted, starving mice try to escape from their territorialized home cage (**Supplementary Fig. 1a, c**), display less aggression toward an intruding conspecific, are less anxious, and engage in risky exploration to seek food. This shift in behavior is accompanied by a coincident change in AgRP neuron activity. In the

absence of food, AgRP neurons are activated by interoceptive cues of negative energy balance, but when food or food-related cues are present, AgRP neuron activity is rapidly silenced [18, 50]. We demonstrate that a subset of AgRP neurons can evoke GABA-mediated inhibition of the MeA and argue that this circuit is responsible for modulating aggressive territorial behavior when food is limited. If food is discovered during foraging, this cue should rapidly relieve GABA-mediated AgRP inhibition of the MeA, providing a switch to adjust behavior for food acquisition. This behavioral switch is difficult to model in the confines of a small arena and isolated housing conditions. When food was presented to hungry residents (artificially induced by AgRP neuron-stimulation) during an intruder trial, they choose to eat rather than interact with the intruder (**Supplementary Fig. 3**). Fluctuations in territorial aggression levels with respect to a limited or depleted food source could be evaluated with the development of techniques to study and track individual animals in a large, group-housed arena.

We propose that the $AgRP^{MeA}$ circuit is involved in territorial adaptations during starvation, but questioned whether hunger itself could influence territorialism. In this experiment we targeted the $AgRP^{PVH}$ circuit which has been demonstrated to evoke robust feeding behavior, equivalent to that following a fast. Unlike activating $AgRP^{MeA}$ fibers, stimulation of the $AgRP^{PVH}$ circuit did not reduce territorial aggression (**Fig. 2g**). These data support the idea that hunger itself does not change territorial behavior. We define a pBNST-projecting MeA^{Npy1R} circuit that is downstream of AgRP and can alter territorial behavior. There are, however, many other AgRP targets throughout the brain, and similar to feeding, they may play redundant roles in territorial adaptations.

The behavioral adaptations that occur during starvation facilitate food acquisition and minimize unnecessary energy expenditure, a complex state-change likely attributed to the broad projection profile AgRP neurons throughout the brain. Not all anatomically distinct AgRP subsets contribute equally to food-intake behavior. Optogenetic stimulation of AgRP fibers in the PVH evokes maximal food consumption, while stimulation of AgRP fibers in the paraventricular thalamus and parabrachial nucleus

302 evoke lesser, if any, influence on food consumption [17, 30]. Similarly, we find that AgRP fibers in the MeA
303 can evoke food intake, but the magnitude of this effect is much less compared to equivalent fiber
304 stimulation in the PVH. The long-term consequence of inhibiting cells in the MeA is a significant increase
305 in body weight (our data and ref [32]). One idea to resolve the differing degrees of food consumption
306 observed by activating distinct AgRP neuron target regions is that their contributions are additive;
307 however, because PVH stimulation is equivalent to stimulating AgRP cell bodies, that explanation is
308 unlikely. Instead, brain regions where AgRP-axon stimulation promotes less food consumption may help
309 coordinate non-feeding behaviors with hunger. For example, AgRP-mediated inhibition of the MeA
310 induces feeding and suppresses territorialism, providing a circuit that can function independently to
311 coordinate two behaviors. It is also possible that under some conditions, select populations of AgRP
312 neurons become activated. The potential for AgRP neurons to orchestrate a complex behavioral
313 response is broad. Future studies detailing the behavioral and physiological contribution of other AgRP
314 targets will provide a complete profile of the starved-state behavioral response.

METHODS

Methods and associated references are available in the online version of this paper.

ACKNOWLEDGMENTS

We thank K. Kafer and M. Chiang for technical assistance generating the new line of mice and maintaining the mouse colonies. We thank M.A. Patterson, and B.C. Jarvie for careful reading of this paper and the entire Palmiter laboratory for helpful discussions and critiques. We thank D.J. Anderson and L. Lo for generously providing H129Δ-fs-TK-TT. We thank E. Strakbein at U.W. Scientific Instruments for the development of tools and apparatuses used in this manuscript. This work was supported by funds from the Hilda Preston Davis Foundation (SLP); the National Institutes of Health (R01DK068098; MJK&OKR), (R01MH094536; LSZ) and (R01DA024908; RDP); Marie Sklodowska-Curie award (H2020-MSCA-IF-2014-658352; ES); AQ is a Ramón y Cajal fellow (RyC-2012-11873) and is funded by European Research Council Starting grant NEUROMITO (ERC-2014-StG-638106) and MINECO Proyectos I+D de Excelencia (SAF2014-57981P)

AUTHOR CONTRIBUTIONS

SLP designed the study under the guidance of RDP; CZ performed and analyzed electrophysiological data in the laboratories of MJK and OKR; MES performed and analyzed electrophysiology data in the laboratory of LSZ; ES performed the RiboTag pulldown and qPCR in the laboratory of AQ; CCN performed single-cell PCR on harvested cells post whole-cell recordings; RDP generated the *AgRP*^{Cre} and *Npy1r*^{Cre} lines of mice; FDB assisted with behavior experiments and blind scoring; RDP, MJK, OKR and LSZ provided laboratory space and resources to conduct the experiments; SLP and RDP wrote the manuscript with revisions and input from all contributing authors.

COMPETING FINANCIAL INTERESTS

The authors declare no competing financial interests.

REFERENCES

1. Sih, A. Optimal Behavior - Can Foragers Balance 2 Conflicting Demands. *Science* **210**, 1041-1043 (1980).
2. Krebs, J.R. Optimal Foraging, Predation Risk and Territory Defense. *Ardea* **68**, 83-90 (1980).
3. Brown, J.L. Citation Classic - the Evolution of Diversity in Avian Territorial Systems. *Cc/Agr Biol Environ*, 16-16 (1981).
4. Anderson, P.K. Foraging Range in Mice and Voles - the Role of Risk. *Can J Zool* **64**, 2645-2653 (1986).
5. Magnhagen, C. Predation Risk and Foraging in Juvenile Pink (Oncorhynchus-Gorbuscha) and Chum Salmon (O-Keta). *Can J Fish Aquat Sci* **45**, 592-596 (1988).
6. Kohler, S.L. & Mcpeek, M.A. Predation Risk and the Foraging Behavior of Competing Stream Insects. *Ecology* **70**, 1811-1825 (1989).
7. Whitham, J. & Mathis, A. Effects of hunger and predation risk on foraging behavior of graybelly salamanders, Eurycea multiplicata. *J Chem Ecol* **26**, 1659-1665 (2000).
8. Wang, L. & Anderson, D.J. Identification of an aggression-promoting pheromone and its receptor neurons in Drosophila. *Nature* **463**, 227-231 (2010).
9. Hahn, T.M., Breininger, J.F., Baskin, D.G. & Schwartz, M.W. Coexpression of Agrp and NPY in fasting-activated hypothalamic neurons. *Nat Neurosci* **1**, 271-272 (1998).
10. Krashes, M.J., Shah, B.P., Koda, S. & Lowell, B.B. Rapid versus delayed stimulation of feeding by the endogenously released AgRP neuron mediators GABA, NPY, and AgRP. *Cell Metab* **18**, 588-595 (2013).
11. Luquet, S., Perez, F.A., Hnasko, T.S. & Palmiter, R.D. NPY/AgRP neurons are essential for feeding in adult mice but can be ablated in neonates. *Science* **310**, 683-685 (2005).
12. Krashes, M.J*., et al.* Rapid, reversible activation of AgRP neurons drives feeding behavior in mice. *J Clin Invest* (2011).
13. Aponte, Y., Atasoy, D. & Sternson, S.M. AGRP neurons are sufficient to orchestrate feeding behavior rapidly and without training. *Nat Neurosci* **14**, 351-355 (2011).
14. Horvath, T.L., Bechmann, I., Naftolin, F., Kalra, S.P. & Leranth, C. Heterogeneity in the neuropeptide Y-containing neurons of the rat arcuate nucleus: GABAergic and non-GABAergic subpopulations. *Brain Res* **756**, 283-286 (1997).
15. Broberger, C., Johansen, J., Johansson, C., Schalling, M. & Hokfelt, T. The neuropeptide Y/agouti gene-related protein (AGRP) brain circuitry in normal, anorectic, and monosodium glutamate-treated mice. *Proc Natl Acad Sci U S A* **95**, 15043-15048 (1998).
16. Cowley, M.A*., et al.* Leptin activates anorexigenic POMC neurons through a neural network in the arcuate nucleus. *Nature* **411**, 480-484 (2001).
17. Betley, J.N., Cao, Z.F., Ritola, K.D. & Sternson, S.M. Parallel, redundant circuit organization for homeostatic control of feeding behavior. *Cell* **155**, 1337-1350 (2013).
18. Betley, J.N*., et al.* Neurons for hunger and thirst transmit a negative-valence teaching signal. *Nature* (2015).

19. Padilla, S.L., Carmody, J.S. & Zeltser, L.M. Pomc-expressing progenitors give rise to antagonistic neuronal populations in hypothalamic feeding circuits. *Nat Med* **16**, 403-405 (2010).
20. Liu, H.*, et al.* Transgenic mice expressing green fluorescent protein under the control of the melanocortin-4 receptor promoter. *J Neurosci* **23**, 7143-7154 (2003).
21. Kishi, T.*, et al.* Expression of melanocortin 4 receptor mRNA in the central nervous system of the rat. *J Comp Neurol* **457**, 213-235 (2003).
22. Stowers, L., Cameron, P. & Keller, J.A. Ominous odors: olfactory control of instinctive fear and aggression in mice. *Curr Opin Neurobiol* **23**, 339-345 (2013).
23. Pereno, G.L., Balaszczuk, V. & Beltramino, C.A. Detection of conspecific pheromones elicits fos expression in GABA and calcium-binding cells of the rat vomeronasal system-medial extended amygdala. *J Physiol Biochem* **67**, 71-85 (2011).
24. Lin, D.*, et al.* Functional identification of an aggression locus in the mouse hypothalamus. *Nature* **470**, 221-226 (2011).
25. Hong, W., Kim, D.W. & Anderson, D.J. Antagonistic Control of Social versus Repetitive Self-Grooming Behaviors by Separable Amygdala Neuronal Subsets. *Cell* **158**, 1348-1361 (2014).
26. Armbruster, B.N., Li, X., Pausch, M.H., Herlitze, S. & Roth, B.L. Evolving the lock to fit the key to create a family of G protein-coupled receptors potently activated by an inert ligand. *Proc Natl Acad Sci U S A* **104**, 5163-5168 (2007).
27. Dietrich, M.O., Zimmer, M.R., Bober, J. & Horvath, T.L. Hypothalamic Agrp neurons drive stereotypic behaviors beyond feeding. *Cell* **160**, 1222-1232 (2015).
28. Laundre, J.W. How large predators manage the cost of hunting. *Science* **346**, 33-34 (2014).
29. Boyden, E.S., Zhang, F., Bamberg, E., Nagel, G. & Deisseroth, K. Millisecond-timescale, genetically targeted optical control of neural activity. *Nat Neurosci* **8**, 1263-1268 (2005).
30. Atasoy, D., Betley, J.N., Su, H.H. & Sternson, S.M. Deconstruction of a neural circuit for hunger. *Nature* **488**, 172-177 (2012).
31. Liu, J., Garza, J.C., Li, W. & Lu, X.Y. Melanocortin-4 receptor in the medial amygdala regulates emotional stress-induced anxiety-like behaviour, anorexia and corticosterone secretion. *Int J Neuropsychopharmacol* **16**, 105-120 (2013).
32. King, B.M., Cook, J.T., Rossiter, K.N. & Rollins, B.L. Obesity-inducing amygdala lesions: examination of anterograde degeneration and retrograde transport. *Am J Physiol Regul Integr Comp Physiol* **284**, R965-982 (2003).
33. Xu, P.*, et al.* Estrogen receptor-alpha in medial amygdala neurons regulates body weight. *J Clin Invest* **125**, 2861-2876 (2015).
34. Lin, S., Boey, D. & Herzog, H. NPY and Y receptors: lessons from transgenic and knockout models. *Neuropeptides* **38**, 189-200 (2004).
35. Sanz, E.*, et al.* Cell-type-specific isolation of ribosome-associated mRNA from complex tissues. *Proc Natl Acad Sci U S A* **106**, 13939-13944 (2009).
36. Heimer-McGinn, V., Murphy, A.C., Kim, J.C., Dymecki, S.M. & Young, P.W. Decreased dendritic spine density as a consequence of tetanus toxin light chain expression in single neurons in vivo. *Neurosci Lett* **555**, 36-41 (2013).
37. Han, S., Soleiman, M., Soden, M.E., Zweifel, L.S. & Palmiter, R.D. A neural circuit for aversive teaching signal during associative learning. *Cell* **(in press)** (2015).
38. Lo, L. & Anderson, D.J. A cre-dependent, anterograde transsynaptic viral tracer for mapping output pathways of genetically marked neurons. *Neuron* **72**, 938-950 (2011).
39. Swanson, L.W. Cerebral hemisphere regulation of motivated behavior. *Brain Res* **886**, 113-164 (2000).
40. Canteras, N.S., Simerly, R.B. & Swanson, L.W. Organization of projections from the medial nucleus of the amygdala: a PHAL study in the rat. *J Comp Neurol* **360**, 213-245 (1995).

41. Niimi, K*., et al.* Heterogeneous electrophysiological and morphological properties of neurons in the mouse medial amygdala in vitro. *Brain Res* **1480**, 41-52 (2012).
42. Bian, X. Physiological and morphological characterization of GABAergic neurons in the medial amygdala. *Brain Res* **1509**, 8-19 (2013).
43. Keshavarzi, S., Sullivan, R.K., Ianno, D.J. & Sah, P. Functional properties and projections of neurons in the medial amygdala. *J Neurosci* **34**, 8699-8715 (2014).
44. Cruikshank, S.J., Urabe, H., Nurmikko, A.V. & Connors, B.W. Pathway-specific feedforward circuits between thalamus and neocortex revealed by selective optical stimulation of axons. *Neuron* **65**, 230-245 (2010).
45. Sun, Q.Q., Akk, G., Huguenard, J.R. & Prince, D.A. Differential regulation of GABA release and neuronal excitability mediated by neuropeptide Y1 and Y2 receptors in rat thalamic neurons. *J Physiol* **531**, 81-94 (2001).
46. Sun, Q.Q., Huguenard, J.R. & Prince, D.A. Neuropeptide Y receptors differentially modulate G-protein-activated inwardly rectifying K+ channels and high-voltage-activated Ca2+ channels in rat thalamic neurons. *J Physiol* **531**, 67-79 (2001).
47. Bosch, M.A., Tonsfeldt, K.J. & Ronnekleiv, O.K. mRNA expression of ion channels in GnRH neurons: subtype-specific regulation by 17beta-estradiol. *Mol Cell Endocrinol* **367**, 85-97 (2013).
48. Behbehani, M.M. Functional characteristics of the midbrain periaqueductal gray. *Prog Neurobiol* **46**, 575-605 (1995).
49. Kennedy, A*., et al.* Internal States and Behavioral Decision-Making: Toward an Integration of Emotion and Cognition. *Cold Spring Harb Symp Quant Biol* **79**, 199-210 (2014).
50. Chen, Y., Lin, Y.C., Kuo, T.W. & Knight, Z.A. Sensory detection of food rapidly modulates arcuate feeding circuits. *Cell* **160**, 829-841 (2015).

FIGURE LEGENDS

Figure 1 AgRP stimulation recapitulates fasting-related foraging and reduced territorialism. (**a**) Schematic diagram of the Pavlovian food-challenge assay used to assess risk taking. (**b**) Viral construct: AAV1-DIO-hM3Dq:mCh, and diagram of the stereotaxic injection site in *Agrp*^{Cre} mice. (**c**) Viral expression of hM3Dq:mCh in AgRP neurons in conjunction with CNO-induced FOS immunoreactivity; scale bar, 100 μm. Animals included in the study (red dots) consumed >1.0 g of food 4 hr post CNO (1 mg/kg IP). (**d**) Post-conditioning (TD) quantification of time spent in the shock-associated chamber (ad lib, *n* = 15; fasted food available, *n* = 7; fasted food blocked, *n* = 7; mCH + CNO, *n* = 13; hM3Dq + CNO food available, *n* = 6; hM3Dq + CNO food blocked, *n* = 7). (**e**) Time spent in the open arms of a plus maze (ad lib, *n* = 8; fasted, *n* = 7; mCH + CNO, *n* = 12; hM3Dq + CNO, *n* = 8). (**f**) Paired analysis of home-cage aggressive behavior (ad lib/fasted paired *n* = 12; hM3Dq + saline/CNO paired, *n* = 10). (**d-f**) Bar outlines indicate mouse genotype: red indicates *Agrp*^{Cre}, while black indicates C57BL/6. The condition or treatments of the animals are indicated below the x-axis. (**d, e**) Conducted during the light cycle (5:00 – 17:00), (**f**) Conducted in the dark (17:00 – 19:00).

Figure 2 MeA-projecting AgRP neurons evoke hunger and inhibit territorial aggression. (**a**) ChR2:YFP-expressing AgRP fibers observed in the MeA. Scale bar, 200 μm. (**b**) Whole-cell, patch clamp recordings (voltage-clamp, -70 mV) of MeA cells in proximity to AgRP::ChR2-expressing fibers. Light-evoked responses were measured with 10-ms light pulse (472 nm, 10 mW power at the tip) in the presence of CNQX and APV (black trace), followed by picrotoxin (red trace). (**c**) Green fluorescent RetroBeads injected into MeA were retained in 7.1 ± 0.6 % of Npy-expressing ARH cells; indicated by arrows. Scale bar, 100 μm. (**d**) Sechmatic demonstrating that a subset of AgRP neurons (black filled) project to the MeA. (**e**) Bilateral injection of AAV1-DIO-ChR2:YFP into the ARH with duel fiber optic cannulas implanted above either the MeA or PVH. (**f**) Stimulation paradigm for behavioral studies: 10 Hz, 5-ms pulse, 5 s on, 2 s off. (**g**) Paired analysis of home-cage aggressive behavior, comparing light on versus light off conditions (MeA fibers, *n* = 8; PVH fibers, *n* = 9); conducted during the first 2 hr of the dark cycle (17:00 – 19:00). (**h**), Cumulative food intake (ChR2 off *n* = 17; ChR2 stimMeA, *n* = 8; ChR2 stimPVH, *n* = 9), measured during the light cycle (10:00 – 14:00)

Figure 3 Npy1R neurons in the MeA can evoke aggression and inhibit feeding. (**a**) Npy1rCre:GFP knock-in targeting construct (diagram not to scale; see methods for complete details). (**b**) RiboTag mice contain a Cre-dependent epitope-taged polyribosome gene. MeA tissue was harvested (red circles) from Npy1rCre; RiboTag mice. (**c**) Comparison of transcripts expressed in precipitated/RiboTagged cells versus those expressed in non-Cre-expresing MeA cells, demonstrated enrichment of *Npy1r* and *Cre* transcripts along with *Gad2* and *Mc4r*. (**d**) Npy1R expression in the anterior-dorsal (AD) and anterior-ventral (AV) MeA; lower, posterior-dorsal (PD) and posterior-ventral (PV) MeA. Scale bar, 200 μm. (**e**) Bilateral injection of AAV1-DIO-hM3Dq:YFP into the MeA of *Npy1r*^{Cre} mice; histology demonstrating the injection site and Cre-dependent YFP fluorescence. Scale bar, 200 μm. (**f**) Stimulation of Npy1RMeA cells of resident animals evokes aggressive behavior (assessed during between 17:00 – 19:00) and (**g**) decreased food consumption (recorded from 17:00 – 21:00; hM3Dq + CNO, *n* = 9; YFP + CNO, *n* = 8) (**h**) Bilateral injection of AAV1-DIO-GFP:TetTox into the MeA of *Npy1r*^{Cre} mice with histology to demonstrate the injection site. (**i - k**) Npy1R^{MeA} neuron silencing did not change home-cage aggression (**f**), but increased body weight (**g**). TetTox-silenced mice also presented decreased threat avoidance behavior (**h**). Conditioned avoidance was measured by time spent in the shock-associated side, on test day (detailed in **Fig. 1a**; TetTox, *n* = 6; YFP, *n* = 6).

Figure 4 The posterior BNST is a secondary target of AgRP and receives direct input from *Npy1R*^{MeA} neurons. (**a**) Injection of AAV1-DIO-Synaptophysin:YFP into the MeA of *Npy1r*^{Cre} mice. (**b**) Immuno-reactive YFP fibers in the: AOBmi (accessory olfactory bulb, mitral layer), LSr (lateral septal nucleus, rostroventral part), PO (preoptic area), pBNST (bed nucleus of the stria terminalis, posterior division, principle nucleus), RCH (retrochiasmatic area), LHA (lateral hypothalamic area), VMH (ventromedial hypothalamus), MeA (medial amygdala), PAG (periaqueductal gray), PB (parabrachial nucleus), NTS (nucleus of the solitary tract). All images were scaled equally; scale bar, 200 μm (see breg -1.6). (**c**) AgRP neurons relay information to the pBNST and MeA. The trans-synaptic virus, H129Δ-fs-TK-TT, was injected into the ARH of *Agrp*^{Cre} mice (top panel). Immunoreacive DsRed cells were present in the MeA (middle panel) and pBNST (bottom panel). Scale bar, 200 μm. (**d**) The MeA relays signals from AgRP neurons to the pBNST. Diagram shows co-injection of green RetroBeads into the pBNST and H129Δ-fs-TK-TT into the ARH of *Agrp*^{Cre} mice. DsRed immune-reactive cell bodies and retrobead-positive cells are present in the MeA. Scale bar, 100 μm. (**e**) Model of the AgRP^{MeA} circuit.

Figure 5 Identification of Vgat-expressing NPY-responsive cells in the MeA that received direct input from AgRP neurons and project to the pBNST. (**a**) Sagittal diagram of injection and recording sites. (**b**) Coronal sections confirming targeted injections of RetroBeads into the pBNST (left) and DIO-ChR2:YFP into the ARH (center). Recordings were performed on bead-labeled cells in the MeA (right); zoom image (right) represents a red cell in proximity to YFP fibers. (**c**) Voltage response to current step injections. The majority of bead-positive neurons exhibited a prominent hyperpolarization-activated voltage sag (h-current; *n* = 10; arrow) and a T type calcium current (*n* = 7; arrow head). (**d**) Light-responsive, bead-positive cells in the MeA (*n* = 3); blue light-evoked fast IPSP (black trace) was abolished in the presence of TTX (blue trace), and rescued with the addition of the K+ channel blocker 4-AP (red trace). (**e**) Bead-positive neurons that displayed an outward current in response to bath application of NPY (1 μM; red line) (14.5 ± 4.5 pA; *n* = 4) when held at -60 mV (note, gaps in the trace indicate the voltage ramp interval in **f**). (**f**) IV relationship during a voltage ramp performed on bead-positive, light-responsive cells, before (black) and after (red) NPY application. (**g**) PCR detection of *Slc32a1* (Vgat) cDNA in cell lysates harvested from recorded cells. Reverse-transcribed cDNA from the hypothalamus was used as a positive control, while hypothalamic RNA was tested as the negative control.

Figure 6 Npy1R^{MeA} neurons that project to the pBNST evoke territorialism. (**a**) Unilateral injection of AAV-DIO-ChR2:YFP into the MeA of *Npy1r*^{Cre} mice, with ipsilateral optic cannulas implanted above the pBNST or the VMH. (**b**) Stimulation of NpyR^{MeA} fibers over pBNST increased aggression in a home-cage intruder assay (left panel), while stimulation of fibers over VMH does not (right panel); VMH, *n* = 3, pBNST, *n* = 5, assessed during the dark cycle (17:00 – 19:00). (**c**) Neither VMH nor pBNST-projecting Npy1R^{MeA} cells decreased feeding (recorded from 17:00 – 21:00).

Figure 1 (Padilla et al.)

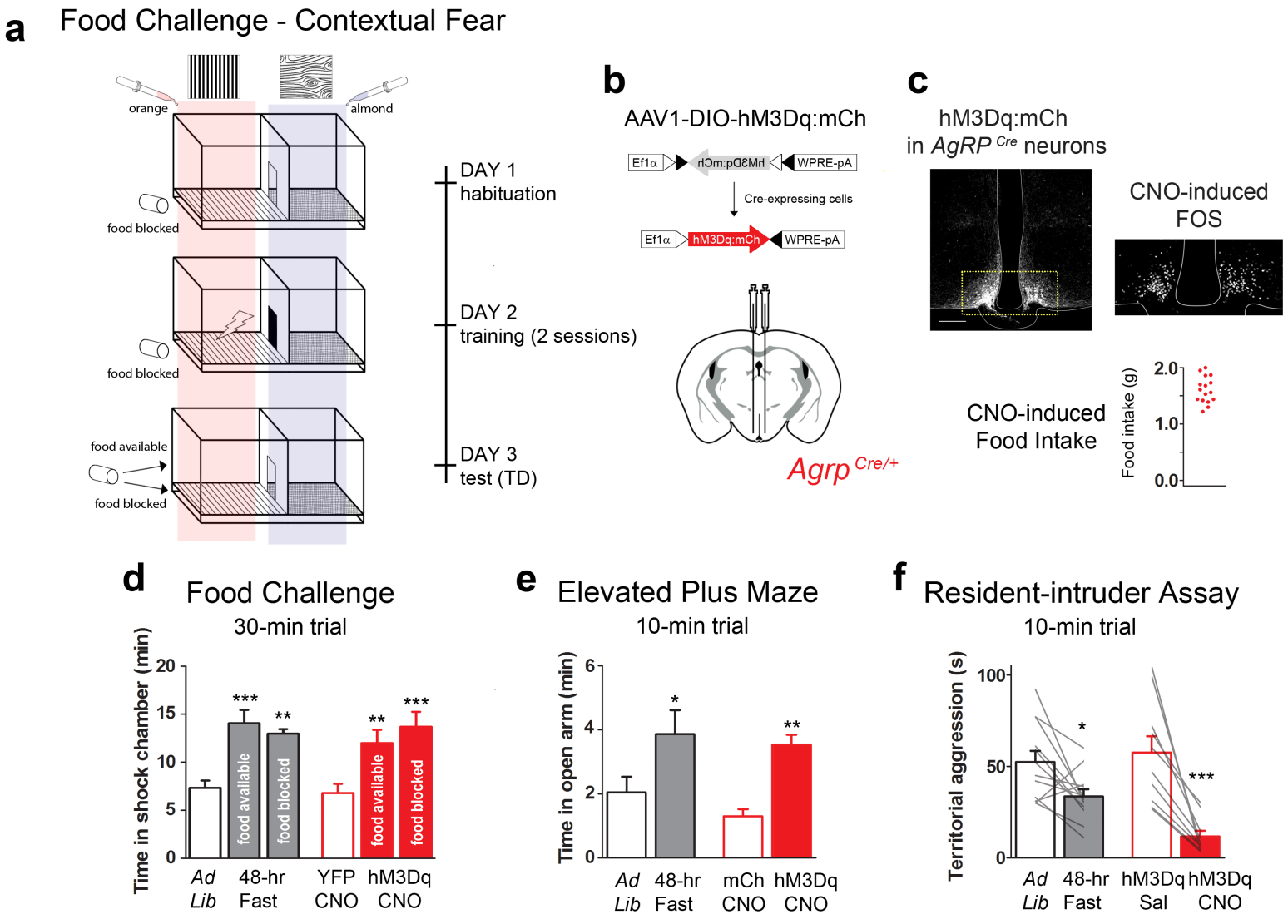

Figure 2 (Padilla et al.)

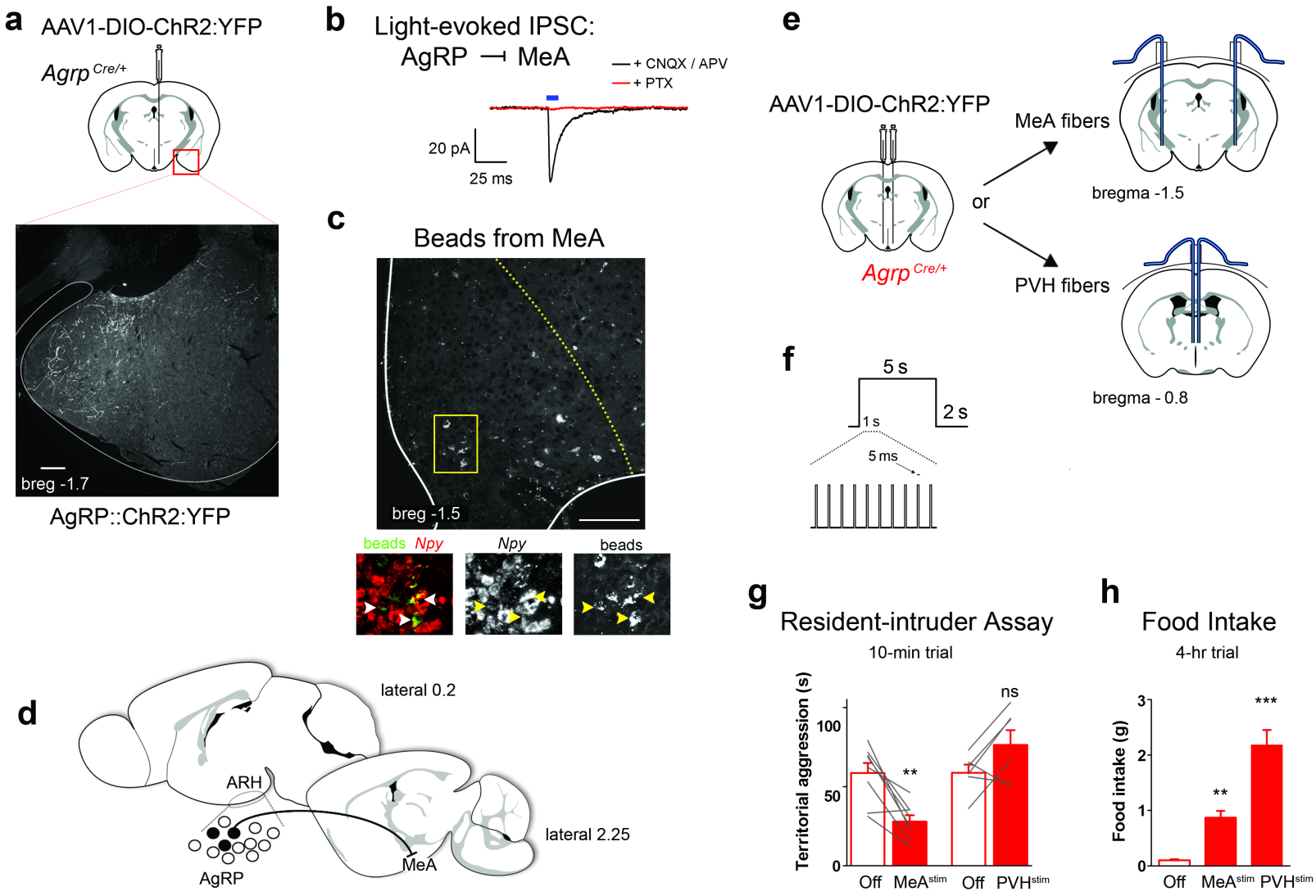

Figure 3 (Padilla et al.)

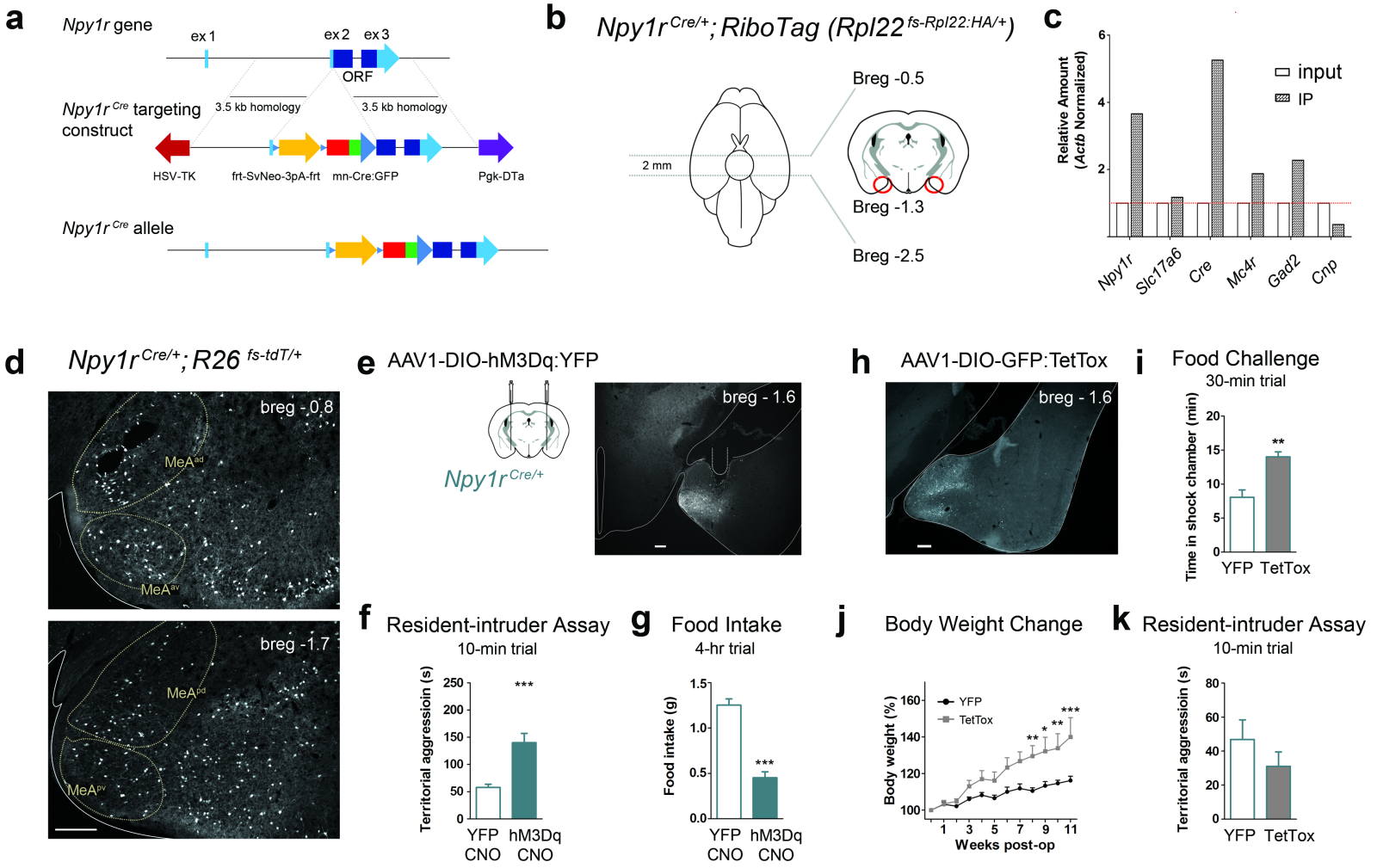

Figure 4 (Padilla et al.)

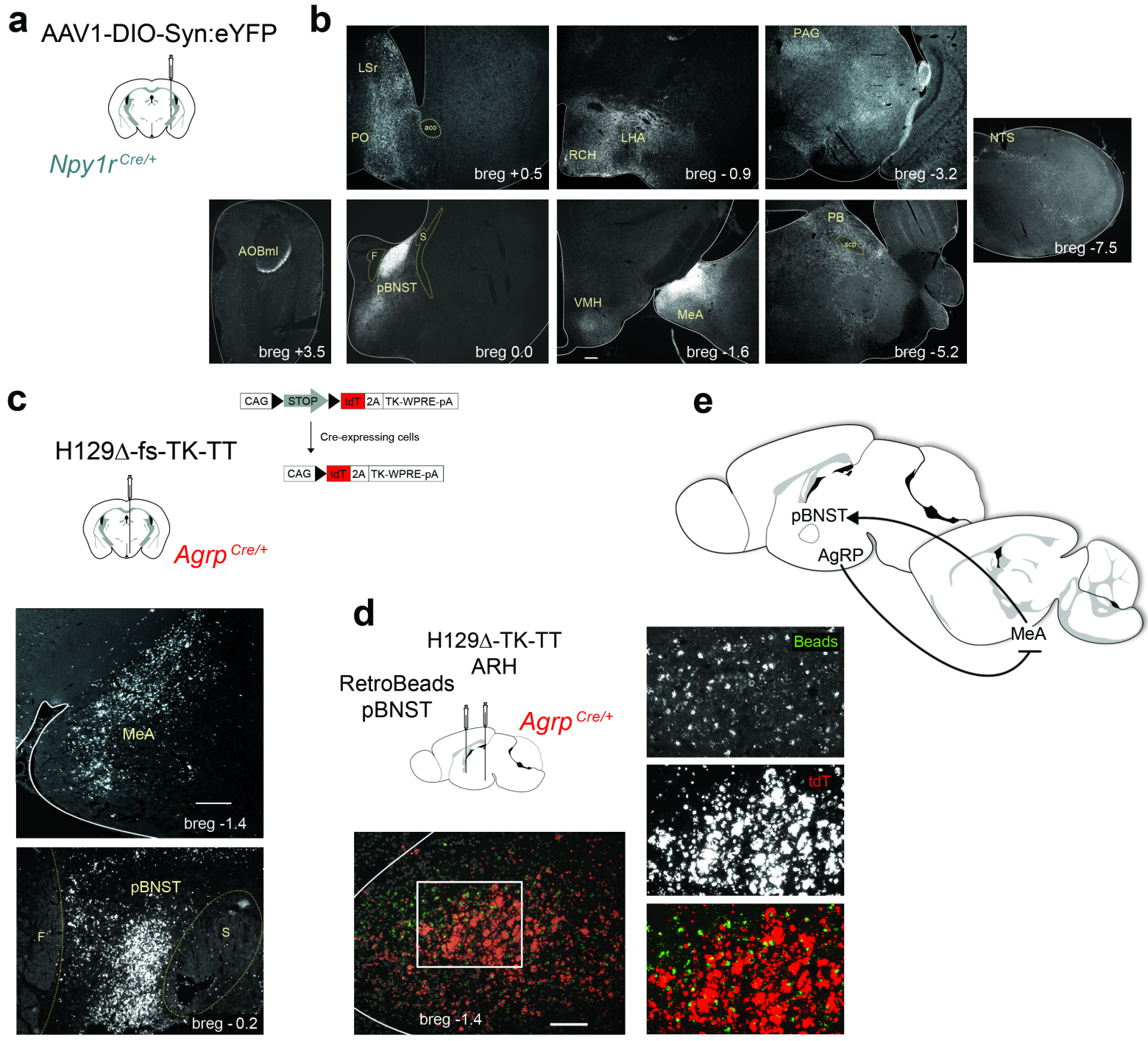

Figure 5 (Padilla et al.)

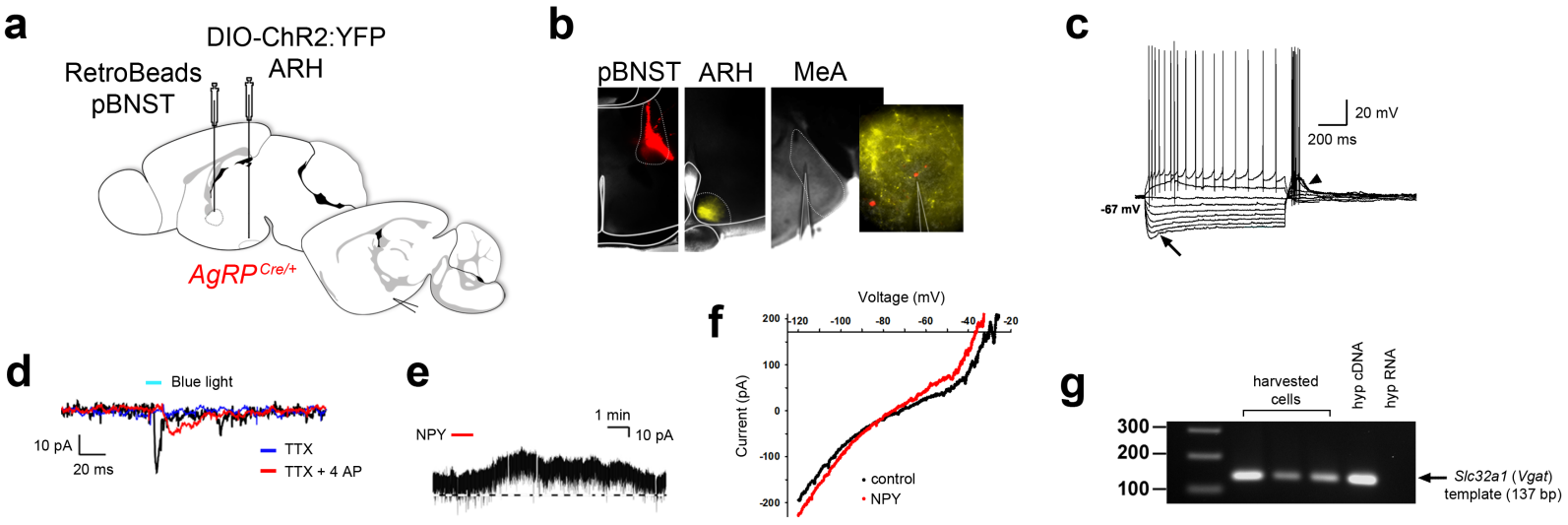

Figure 6 (Padilla et al.)